Applied Energy 227 (2018) 220–230

Contents lists available at ScienceDirect

Applied Energy

journal homepage: www.elsevier.com/locate/apenergy

Performance evaluation of a low-grade power generation system with CO_2 transcritical power cycles

Y.T. Ge[a,*], L. Li[a], X. Luo[b], S.A. Tassou[a]

[a] RCUK National Centre for Sustainable Energy Use in Food Chains (CSEF), Institute of Energy Future, Brunel University London, Uxbridge, Middlesex UB8 3PH, UK
[b] National Key Laboratory of Science and Technology on Aero Engines Aero-thermodynamics, The Collaborative Innovation Centre for Advanced Aero-Engine of China, Beihang University, Beijing 10191, China

HIGHLIGHTS

- Experiment in a power generation system with CO_2 transcritical power cycles (T-CO_2).
- Preliminary test results from the T-CO_2 power generation system.
- Model development and validation of the tested T-CO_2 power generation system.
- Some important operating parameters on system performance are identified.
- The research outcomes can be used to instruct the system control and operation.

ARTICLE INFO

Keywords:
CO_2 transcritical rankine cycles
CO_2 power generation system
Experimental investigation
Modelling

ABSTRACT

Globally, there are vast amounts of low-grade heat sources from industrial waste and renewables that can be converted into electricity through advanced thermodynamic power cycles and appropriate working fluids. In terms of the working fluid's environmental impact, temperature match of cycle heat processes and system compactness, CO_2 transcritical power cycles (T-CO_2) were deemed more applicable for low-grade heat to power conversion. However, the system thermal efficiency of a T-CO_2 requires further improvement. Subsequently, a test rig of the small-scale power generation system with T-CO_2 power cycles was developed with essential connected components. These include a plate thermal coil CO_2 supercritical heater, a CO_2 transcritical turbine, a plate recuperator, an air-cooled finned-tube CO_2 condenser and a CO_2 liquid pump. Various preliminary test results from the system measurements are demonstrated in this paper. Meanwhile, the system model has been developed and applied to predict system performance at different operating conditions. The simulation results can therefore instruct further design and optimisation of system and components.

1. Introduction

The extensive consumption of fossil fuels worldwide in power generation has been increasingly contributing towards global warming, air pollution and the imminent energy crisis. One of the challenges of the 21st century is to tackle the risks arising from excessive CO_2 emissions by replacing fossil fuels with recovered waste heat and renewable energy. Waste heat sources can be divided into three main categories according to their temperature ranges: high temperature (> 650 °C), medium temperature (230–650 °C) and low temperature (< 230 °C) [1]. However, statistics have shown that more than 50% of industrial waste heat and renewables are within the low-grade range [2]. These include heat from manufacturing and process industries, solar energy, geothermal energy, and from internal combustion engine exhausts and coolants used in commercial, institutional or automotive applications. Therefore, low-grade waste heat recovery for power generation is a significant and highly recommended strategy to tackle global warming, utilising advanced thermodynamic power cycles and appropriate working fluids [3,4].

Organic Rankine Cycles (ORC) are a known feasible option for the application of low-grade heat sources in terms of operating parameters, system sizes, thermal and exergy efficiencies. The ORC functions similarly to a Clausius-Rankine steam power plant, but instead uses an organic working fluid such as R245fa, which is able to condense at a lower pressure (compared to evaporator pressure) and evaporate at a higher pressure (compared to condenser pressure). However, one

* Corresponding author.
E-mail address: Yunting.Ge@brunel.ac.uk (Y.T. Ge).

http://dx.doi.org/10.1016/j.apenergy.2017.07.086
Received 11 January 2017; Received in revised form 19 July 2017; Accepted 22 July 2017
Available online 04 August 2017

Nomenclature

A	heat transfer area (m^2)
C	product of mass flow rate and specific heat (W/K)
CP	constant pressure specific heat of air (J/kg K)
k	thermal conductivity (W/m K)
L	vertical length of heat exchanger (m)
$\dot{m}$	mass flow rate (kg/s)
N	number of plate
P	pressure (pa)
Q_T	heat capacity (W)
T,t	temperature (°C)
ΔT	temperature difference (K)
U	heat transfer coefficient (W/m^2 K)
UA	overall heat conductance (W/K)
W	power generation (W)

Greek symbols

ε	heat transfer effectiveness (–)
ϕ	length ratio
α	heat transfer coefficient (W/m^2 K)
β	chevron angle
δ	plate thickness (mm)
ρ	density (kg/m^3)
μ	kinematic viscosity (mm^2/s)

Subscripts

air	air
aircd	condenser air inlet
ci	cold fluid inlet
co	cold fluid outlet
exp	expander
expin	expander inlet
hi	hot fluid inlet
ho	hot fluid outlet
max	maximum
min	minimum
oil	thermal oil
p	plate
sc	subcooling

important limitation of the ORC is its constant evaporation temperature, which increases irreversibly during the heat addition process when using sensible heat sources such as waste heat [5]. In addition, a hydrofluorocarbon (HFC) working fluid is conventionally applied in an ORC, which has zero Ozone Depletion Potential (ODP) but a relatively high Global Warming Potential (GWP). This will affect the future application of ORCs in low-grade waste heat recovery.

On the other hand, as a natural working fluid, CO_2 has been widely applied in refrigeration [6] and heat pump [7] systems owing to its zero ODP, negligible GWP and superb thermophysical properties, despite its high critical pressure and low critical temperature. The high operating pressures of a CO_2 energy system require special designs for system components and controls, while the low critical temperature will turn a CO_2 low-grade power generation system into a transcritical Rankine cycle (T-CO_2) or even a supercritical CO_2 Brayton cycle. Of these CO_2 power cycles, the T-CO_2 is most effective at harvesting low-grade heat sources when a low temperature heat sink is accessible [8,9]. The supercritical heat-addition process of a T-CO_2 can produce high-efficiency temperature matching between the sensible heat source and the working fluid, leading to no pinch limitations. In addition, the superb thermophysical properties of CO_2 can create a more compact T-CO_2 system than those of ORCs. These include a higher density, latent heat, specific heat, thermal conductivity, volumetric cooling capacity, and lower viscosity. Therefore, the T-CO_2 has considerable potential for low-grade power generation. Nevertheless, the performance of such a system requires thorough investigation in order to understand operational mechanisms for optimising system efficiency.

Due to the high critical pressures of CO_2, the pressure of heating processes in CO_2 transcritical power cycles would also be high (typically above 90 bar), such that conventional heat exchangers, gas turbines or expanders and power cycles cannot be directly applied. Consequently, up to now, investigations on low temperature heat source energy conversion systems with CO_2 transcritical power cycles have been limited to small-scale laboratory work and theoretical analyses. A solar-powered test rig with a CO_2 transcritical power cycle was set up to examine system performance at designated operating states [10]. As this test rig used a throttling valve to simulate expansion device, power generation could not be measured directly. A highly promising solution to the CO_2 turbine market problem is to use a CO_2 scroll expander for the test rig or practical installation. The expander works as the corresponding compressor in reverse, which is a positive displacement machine. CO_2 scroll expanders and compressors have already been implemented in refrigeration and air conditioning [11]; however, its application in transcritical power cycles needs to be explored as it plays an important role in the power system. A steady-state thermodynamic model for the above solar-CO_2 power system showed that the power and heat outputs and efficiencies varied remarkably in different seasons of the year, due to the periodical change of solar radiation [12]. Therefore, a transient mathematical model would be more suitable in simulating the real performance of the solar system. In the application of waste heat with a maximum heat source temperature of 150 °C, the performance of a CO_2 transcritical power cycle with optimised supercritical pressure was compared thermodynamically to a R123 ORC subcritical cycle [13]. The total system efficiency of the CO_2 transcritical cycle was proven to be higher than that of a R123 subcritical cycle due to better matching of the CO_2 flow temperature variation to its heat source temperature glide. In addition, the CO_2 power system is more compact and the cycle also shows no pinch limitation in the heat exchanger. This result is encouraging since the R123 subcritical cycle was formerly recognised to harbour a higher system performance [14]. Significantly, this research demonstrates the importance of the design and selection of the high side supercritical CO_2 gas heater and optimal supercritical pressure control in order to determine overall system efficiency [15]. However, comprehensive experimental and theoretical analyses for a low-grade T-CO_2 system are necessary to gain full understanding of system operations and achieve optimal designs and controls. So far, to the authors' acknowledges, very few experimental investigations have been carried comprehensively on low-grade power generation with T-CO_2 systems in which actual power generations were measured. On the other hand, some theoretical analyses including energy and exergy were conducted on the T-CO2 systems but mostly were limited to thermodynamics bases [16–19]. Nevertheless, to fully understand and model the system performance and controls, the detailed system component models need to be involved. These issues will be addressed in the paper in terms of comprehensive experimental investigation and detailed model development.

In this paper, a test rig of a low temperature power generation system with the T-CO_2 power cycle is described and measurements demonstrated for the effect of CO_2 mass flow rates and heat source flow rates on system performance. In the meantime, a mathematic model of the tested system was developed and validated with measurements from current and previous research projects. The model predicts the effect of heat sink and source parameters and CO_2 pressures at the turbine inlet on system performance, which aids in the understanding of

system operations towards the eventual optimisation of system design and controls.

2. Experimental investigation

2.1. Test facilities

A test rig of a small-scale low-grade power generation system with T-CO_2 power cycles was purposefully built on the top floor of an 80 kW_e micro-turbine CHP unit, as shown schematically in Fig. 1.

To clearly understand the flow process of the T-CO_2 power cycles, the system layout and its corresponding T-S diagram are depicted in Fig. 2. The test rig consisted of a number of essential components including a CO_2 turbine/expander, electricity generator, recuperator, air-cooled condenser, receiver, liquid pump and thermal oil-heated CO_2 gas generator. The CO_2 turbine is an axial type with single stage. The turbine stage is reaction type with a reaction degree or reaction ratio of 0.5. The turbine designed power generation, pressure ratio, CO_2 mass flow rate and diameter are 5 kWe, 1.5, 0.281 kg/s and 144 mm respectively. The turbine power generation was connected directly to grid and there was no load connected to the turbine. An automatic generation control was therefore applied to control turbine rotational speed. However, the turbine rotational speed was not measured by this project. The CO_2 liquid pump was a type of triplex plunger pump with a minimum power consumption of 3 kW flexibly coupled with an 11 kW motor most suitable for the frequency inverter. The heat source of the test rig was hot thermal oil flow heated by exhaust flue gases from the 80 kW_e CHP unit. The thermal oil parameters, temperature and flow rate were respectively modulated by the CHP power output and a variable-speed thermal oil pump. On the condenser side, the air flow (heat sink) parameters, flow rate and temperature were respectively controlled by a variable-speed condenser fan and a purposely-built electric heater installed underneath the heat exchanger. Inside the T-CO_2 Rankine cycle, the supercritical CO_2 pressure and temperature were varied and controlled by thermal oil side flow rate and temperature respectively, and the CO_2 condensing pressure by heat sink parameters particularly air flow rate. In addition, the CO_2 mass flow rate was modulated by means of a variable speed CO_2 liquid pump which concurrently affected the CO_2 supercritical pressure. Furthermore, four two-way valves were installed at the CO_2 turbine exit and high-pressure liquid line to allow the CO_2 working fluid to either flow through or bypass the recuperator. The system performance with and without the recuperator could therefore be measured and compared.

The test rig was fully instrumented with a temperature sensor and pressure transducer between any two main components in the system. The inlet and outlet temperatures and flow rates of the thermal oil and condenser air flows were all measured. In addition, a CO_2 mass flow meter and electricity power meter were also installed to respectively measure the CO_2 mass flow rate and turbine power generation. These instruments or sensors were completely calibrated before installation to ensure acceptable accuracy, with each thermocouple uncertainty at less than ± 0.5 °C, pressure transducer ± 0.3%, air velocity meter ± 3.0%, CO_2 mass flow rate ± 0.1% and power meter ± 0.8%.

As listed in Table 1, a series of measurements were carried out on the developed test rig at different heat source and sink parameters. For the heat source parameters, temperatures varied between 142.4 °C and 144.4 °C, and the flow rate from 0.25 kg/s to 0.5 kg/s. As for the heat sink parameters, temperatures varied from 22.5 °C to 23.5 °C which can be treated as constant but flow rate remained unchanged. In addition, the CO_2 mass flow rate was controlled by the CO_2 liquid pump in the range of 0.2 kg/s and 0.3 kg/s. The test results can be used to validate the system and component models to be developed.

2.2. Test results

Table 1 demonstrates that for heat source parameters, thermal oil temperatures do not significantly vary; moreover, at the heat sink side, both condenser inlet air temperatures and flow rates remained approximately constant. Therefore, from the test results, only the effects of thermal oil flow rate and CO_2 mass flow rate on system performance have been selected and demonstrated in this paper. It is understandable that CO_2 mass flow rates increased linearly with higher CO_2 liquid pump speeds, and decreased slightly at higher thermal oil flow rates. The test results verify that CO_2 mass flow rates in the T-CO_2 power cycle can be effectively controlled by the modulation of CO_2 pump speeds. Subsequently, the effect of the CO_2 pump speed on system performance can be represented by the CO_2 mass flow rate. As depicted in Fig. 3, both CO_2 pressures at the turbine inlet and outlet increased at higher CO_2 mass flow rates, providing starting pressures were not too low. Moreover, higher thermal oil flow rates could also augment both CO_2

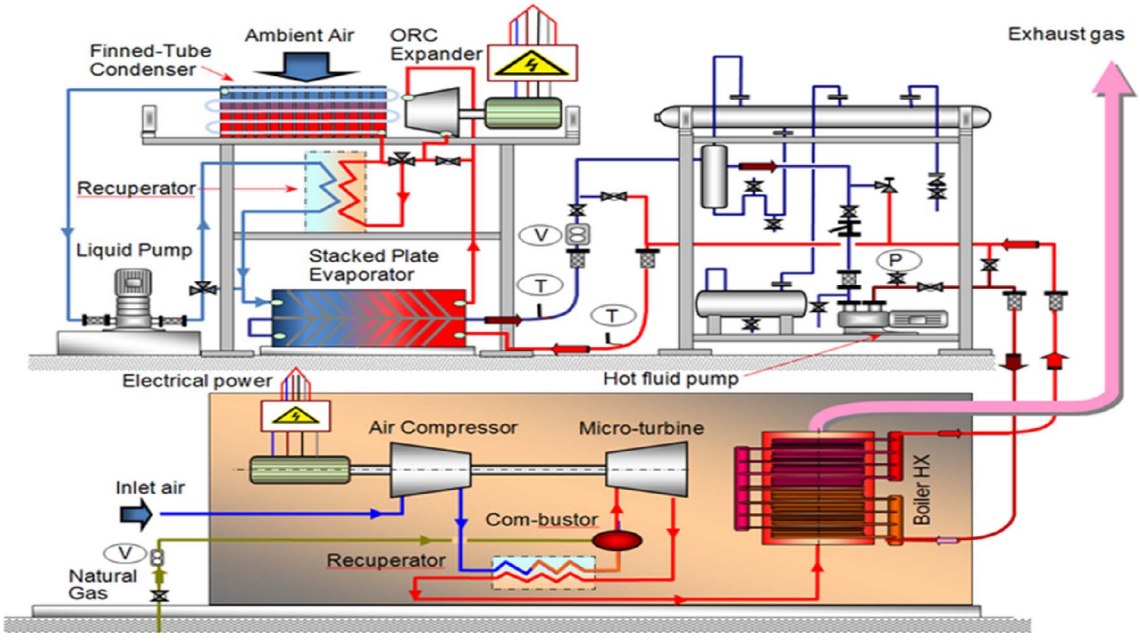

Fig. 1. Test facility of CO_2 transcritical power generation system and its integration with an 80 kW microturbine CHP unit.

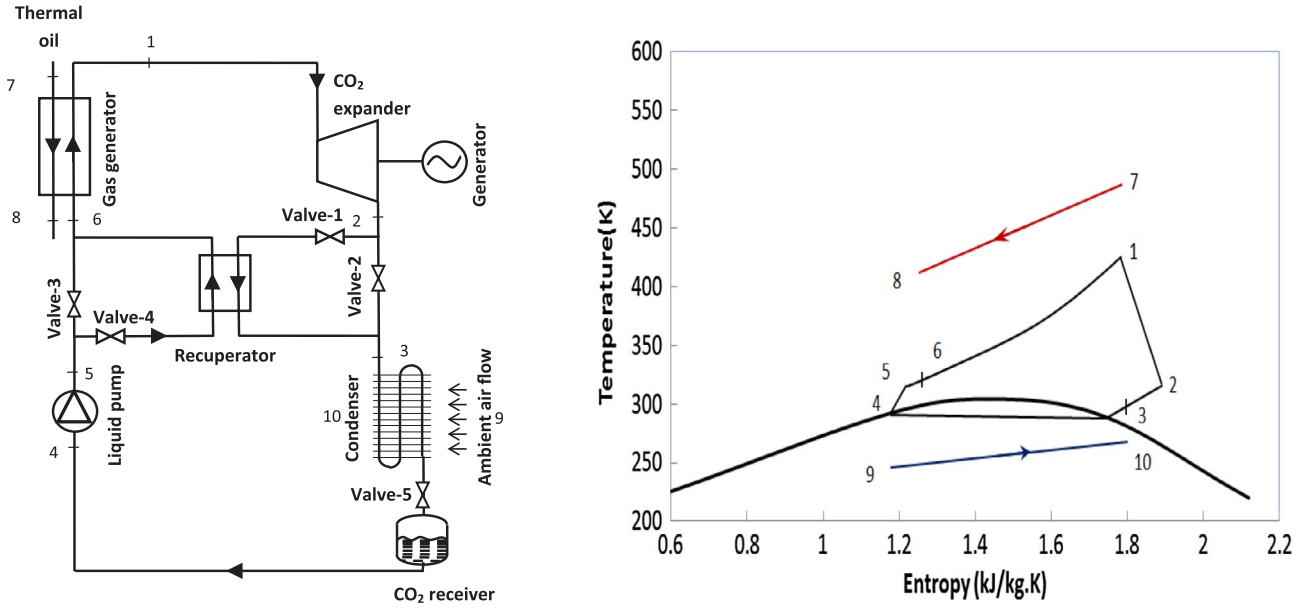

Fig. 2. Schematic diagram of CO_2 power generation test rig and corresponding T-S diagram.

Table 1
Variation of operating parameters for the system test.

Thermal Oil inlet temperature (°C)	Thermal oil flow rate (kg/s)	Condenser inlet air flow temperature (°C)	Condenser inlet Air flow rate (m^3/s)	CO_2 mass flow rate (kg/s)
142.4–144.4	0.25–0.5	22.5–23.5	4.267	0.2–0.3

pressures.

The CO_2 mass flow rate and thermal oil flow rate also exerts an effect on the power generation of the CO_2 turbine, as shown in Fig. 4. There are two groups of results in the figure; the solid lines are derived from turbine generator measurements and the dotted lines represent actual cycle power generations calculated individually from the product of measured CO_2 mass flow rate and the enthalpy difference between the turbine inlet and outlet. The enthalpy at either turbine inlet or outlet is calculated from corresponding measurements of temperature and pressure. The ratio of turbine power generation to actual cycle power generation is a product of turbine mechanical efficiency and electrical efficiency, both of which need to be significantly improved. As seen from the measurements, power generation increases with both higher CO_2 mass flow rates and higher thermal oil flow rates. Accordingly, the turbine isentropic efficiency and overall efficiency are calculated at different CO_2 and thermal oil mass flow rates, as depicted in Fig. 5. The turbine overall efficiency is defined as the product of turbine isentropic efficiency, mechanical efficiency and electrical efficiency. Higher CO_2 mass flow rates have shown to enhance overall turbine efficiency but does not benefit isentropic efficiency, which in turn should be significantly affected by turbine pressure ratio and speed. In addition, higher thermal oil flow rates can reinforce both turbine isentropic and overall efficiencies.

3. Model development and simulation

As seen from Section 2.2, the test results of the T-CO_2 power system are limited because of high operating pressures at the turbine inlet and regular leakage of the CO_2 liquid pump. To fully understand the operations and controls of the tested system, a comprehensive system model for the T-CO_2 power cycle has been developed under the TRNSYS software platform by integrating all of the essential component models, as shown in Fig. 6. These include a CO_2 gas generator, turbine, recuperator, air cooled condenser and liquid pump. It should be noted that the CO_2 finned-tube air cooled condenser model has been previously developed, validated and comprehensively explained by the authors [20]. In brief, the model was developed based on lumped method in which the condenser was divided into three sections: superheat, saturated and subcooled. The calculations of energy balances and pressure drops were applied into each section of the heat

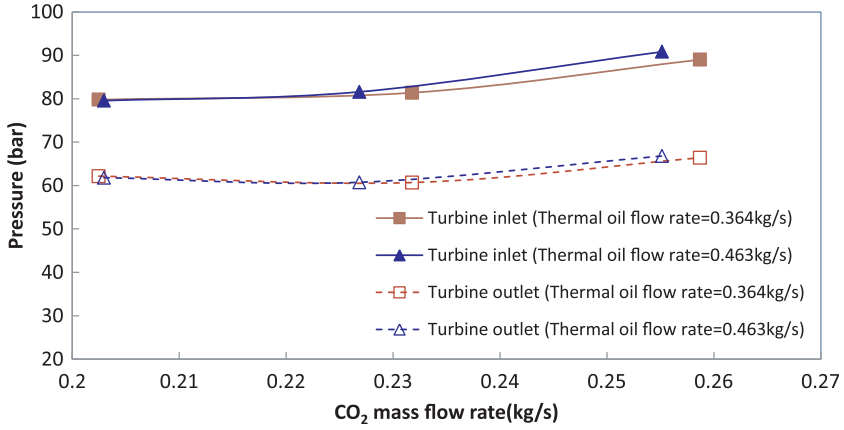

Fig. 3. Variation of CO_2 pressures at turbine inlet and outlet with different CO_2 mass flow rates and heat source flow rates.

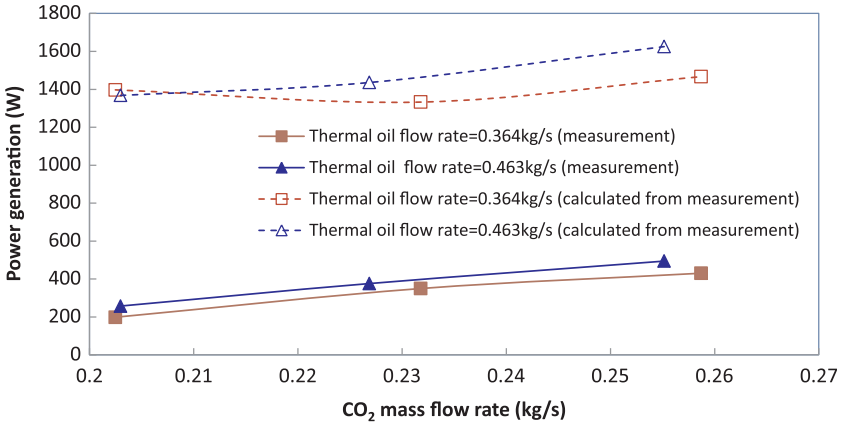

Fig. 4. Variation of turbine power generations with different CO_2 mass flow rates and heat source flow rates.

exchanger. For the models of turbine and liquid pump, conventional thermodynamic models were applied for actual expansion and compression processes. In each of these models, the efficiencies of isentropic, mechanical and electrical are assumed to be constant although certain effective parameters could be considered [21]. Therefore, in this paper, only the component models of CO_2 gas generator and recuperator are described.

3.1. Models of CO_2 gas generator and recuperator

A plate CO_2 gas generator was used in the T-CO_2 test rig in which thermal oil and supercritical CO_2 were respectively positioned on the hot and cold sides of the heat exchanger. The thermal oil was used as a high-temperature heat transfer fluid and heat source for the CO_2 gas generator with a working temperature ranging from 0 to 340 °C. Based on the manufacturer's data, various important thermophysical properties of the thermal oil are correlated and presented respectively in Eqs. (1)–(4).

For density (kg/m^3) at temperature range 0–340 °C:

$$\rho = -0.65035606 \times T + 875.94428 \quad (1)$$

For specific heat capacity (kJ/kg K) at temperature range 0–340 °C:

$$Cp = 0.0036446769 \times T + 1.8087169 \quad (2)$$

For thermal conductivity (W/m K) at temperature range 0–340 °C:

$$k = -7.2360691 \times 10^{-5} \times T + 0.13570055 \quad (3)$$

For kinematic viscosity (mm^2/s) at temperature range 0–340 °C:

$$\mu = 27604.397 \times T^{-1.879364} \quad (4)$$

These properties are important parameters for the heat transfer calculation and analysis of the CO_2 gas generator. On the other hand, a plate recuperator was installed in the rig to evaluate its effect on system performance. As shown in Figs. 1 and 2, the hot and cold sides of the recuperater respectively constitute low pressure CO_2 superheated gas from the turbine exit and high pressure subcooled liquid from the pump outlet. Since there is no phase change for either the CO_2 gas generator and recuperator, the same model may be applied to both heat exchangers and as such, they are described together in this paper.

As shown in Fig. 7, internally, for each plate heat exchanger, many Chevron plates are installed in parallel with a fixed pitch between two neighbour plates. Certain structural parameters describing the heat exchanger are required for the model development [22]. These include the total number of plates (N), channel numbers per pass for both hot and cold fluids, distance between the head plates, horizontal length of the plates (W), vertical length of the fluid path between the upper and lower ports (L_p), plate thickness (δ_p), the ratio of the developed length to the projected length (ϕ) and chevron angle (β), etc.

For the plate heat exchanger, as shown in Fig. 7, counter flow profiles for hot and cold fluids are assumed and the effectiveness ε for the heat transfer is calculated:

$$\varepsilon = \frac{1-\exp\left(-\frac{UA}{C_{\min}}\left(1-\frac{C_{\min}}{C_{\max}}\right)\right)}{1-\left(\frac{C_{min}}{C_{max}}\right)\exp\left(-\frac{UA}{C_{\min}}\left(1-\frac{C_{\min}}{C_{\max}}\right)\right)} \quad (5)$$

where the parameters in the right side of Eq. (5) can be calculated as below:

$$A = L_P \times W \times \varnothing \times N; \quad U = \frac{1}{\frac{1}{\alpha_{hi}} + \frac{1}{\alpha_{ci}}}; \quad UA = U \times A \quad (6)$$

$$C_{hi} = \dot{m}_{hi} CP_{hi}; \quad C_{ci} = \dot{m}_{ci} CP_{ci} \quad (7)$$

$$C_{max} = \text{maximum value of } C_{hi} \text{ and } C_{ci} \quad (8)$$

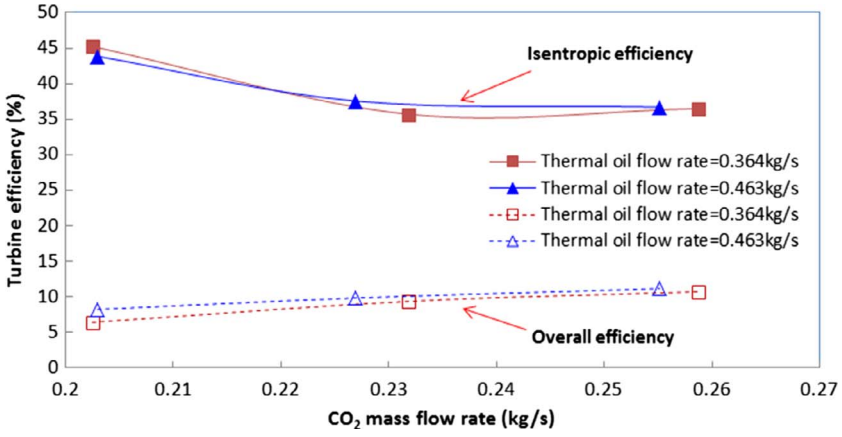

Fig. 5. Variation of turbine efficiencies with different CO_2 mass flow rates and heat source flow rates.

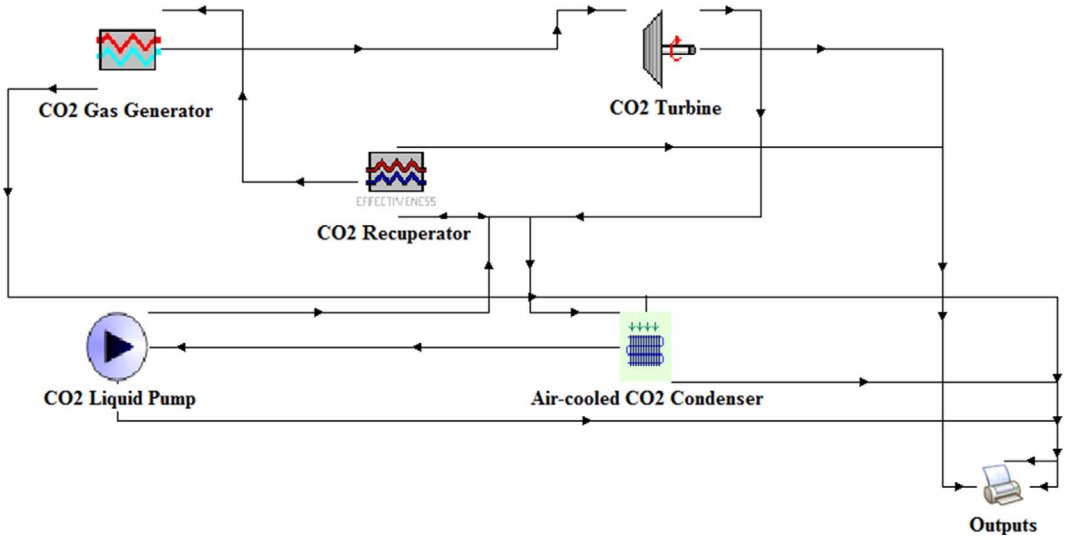

Fig. 6. TRNSYS model of T-CO_2 power generation system.

C_{min} = minimum value of C_{hi} and C_{ci} (9)

The correlations from literature reference are used to calculate the fluid heat transfer coefficients on both hot and cold sides [23].

The heat capacity and fluid outlet temperatures of both hot and cold sides can therefore be calculated.

$$Q_T = \varepsilon C_{min}(T_{hi}-T_{ci}); \quad T_{ho} = T_{hi}-\frac{Q_T}{C_{hi}}; \quad T_{co} = T_{ci}-\frac{Q_T}{C_{ci}} \tag{10}$$

3.2. Model validation

The developed gas generator model is then used to predict the heat exchanger's hot and cold-side outlet parameters and heat capacity when corresponding inlet parameters from measurements are given, as listed in Table 2. The simulation results compared with measurements including thermal oil outlet temperature, CO_2 outlet temperature and the heat exchanger capacity are shown in Figs. 8–10 respectively. The results reveal that thermal oil outlet temperatures tend to be over-predicted by the model while CO_2 outlet temperatures are under-predicted. One of the reasons may stem from the assumption of constant specific heat capacity on the CO_2 side which actually changes significantly during the supercritical heating process in the heat exchanger. However, the predicted temperature errors are mostly within 5 K, which are generally acceptable considering the high temperature ranges of both hot and cold fluids. The temperature prediction errors lead to model under-prediction for the heat exchanger heat capacity compared to measurements, as shown in Fig. 10. Nonetheless, these relative errors are mostly within 5% and again are acceptable. Since the overall test results were achieved under a T-CO_2 power generation system without the recuperator, the validation of the recuperator model could not be carried out. However, considering the similarity between recuperator and gas generator models, the recuperator model is assumed to be reasonable. As explained previously, these can therefore demonstrate the acceptability of the T-CO_2 system model.

Table 2
The test parameter ranges for the hot and cold side inlets of CO_2 gas generator.

Thermal oil inlet parameter range		CO_2 inlet parameter range		
Temperature (°C)	Flow rate (kg/s)	Temperature (°C)	Pressure (bar)	Flow rate (kg/s)
139.0–151.0	0.25–0.5	27.5–33.5	77.0–92.0	0.20–0.27

3.3. Simulation of the T-CO_2 power generation system

The model of the test system with fixed components can thus be used to predict the effects of heat source and sink parameters and CO_2 pressures at the turbine inlet with large scales on system performance. The variations of these parameters are specified in Table 3, in which thermal oil inlet temperatures vary between 200 °C and 280 °C, its flow rate between 0.8 kg/s and 1.6 kg/s, and condenser incoming air temperatures from 5 °C to 25 °C. The temperature difference between CO_2

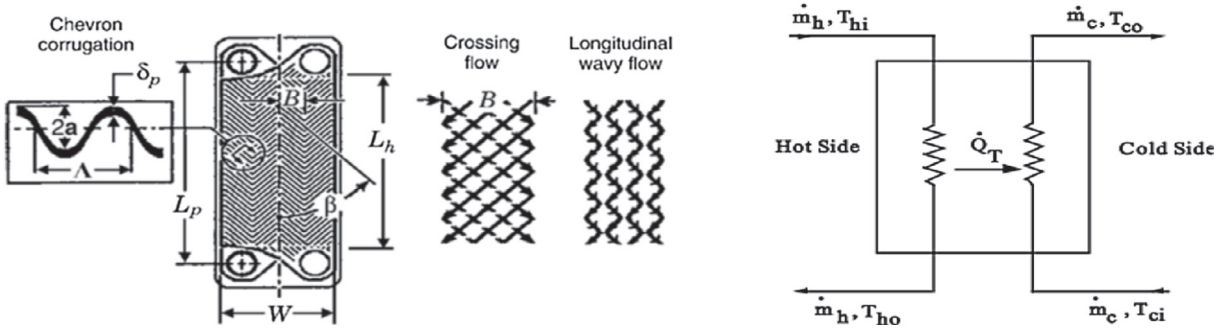

Geometrical parameters of a Chevron plate [17]

A counter flow mode

Fig. 7. Plate parameters and flow mode of the plate heat exchanger.

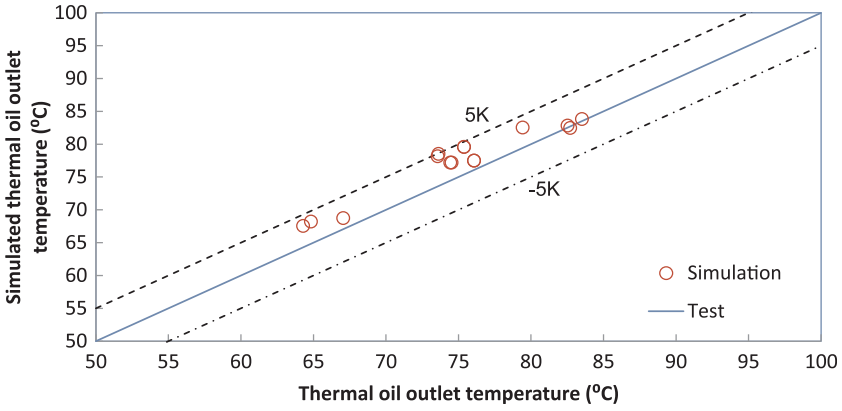

Fig. 8. Comparisons of simulation and test results for thermal oil outlet temperatures of the CO_2 gas generator.

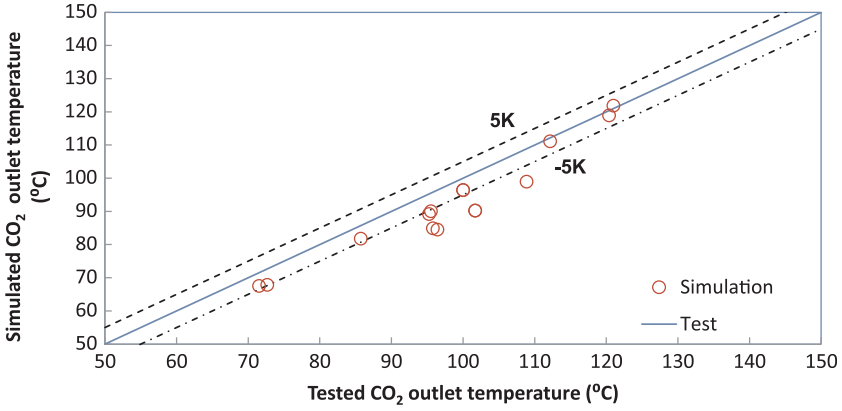

Fig. 9. Comparisons of simulation and test results for CO_2 outlet temperatures of the CO_2 gas Generator.

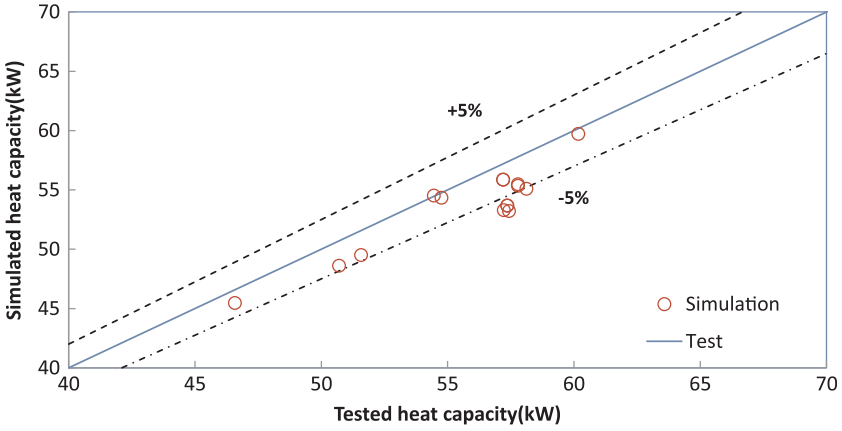

Fig. 10. Comparisons of simulation and test results for heat capacity of the CO_2 gas generator.

Table 3
Operation conditions for model simulation.

Thermal oil side (heat source)		Condenser air side (heat sink)			Turbine inlet	Power generation
t_{oil} (°C)	Flow rate (kg/s)	t_{air} (°C)	ΔT_{sc} (K)	ΔT_{aircd} (K)	P_{expin} (bar)	W_{exp} (kW)
200–280	0.8–1.6	5–25	2	5	80–120	5

condensing and condenser incoming air is assumed constant at 5 K and the CO_2 liquid subcooling at the condenser outlet is controlled at 2 K by modulating the condenser fan speed or condenser air flow rate. The system power generation is designed and specified to 5 kW_e, and can be controlled by the variable speed CO_2 liquid pump or CO_2 mass flow rate in the system at different conditions, while CO_2 pressures at the turbine inlet can be modulated from 80 bar to 120 bar. In a similar strain to the experimental measurement, for each model simulation, only one parameter is changed with all others kept constant at 240 °C thermal oil side temperature, 1.2 kg/s oil flow rate and 120 bar turbine inlet pressure.

Figs. 12 and 13 respectively show the effects of condenser incoming air temperature, thermal oil inlet temperature and flow rate on the CO_2 mass flow rate so as to generate 5 kW power in different conditions. Fig. 11 furthermore demonstrates that at fixed thermal oil side parameters (temperature and flow rate), the CO_2 mass flow rate should be

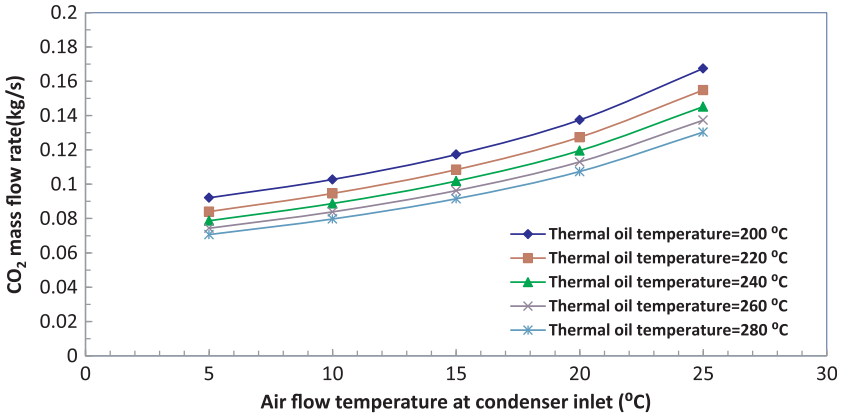

Fig. 11. Variation of CO_2 mass flow rate with thermal oil temperature and condenser inlet air Temperature.

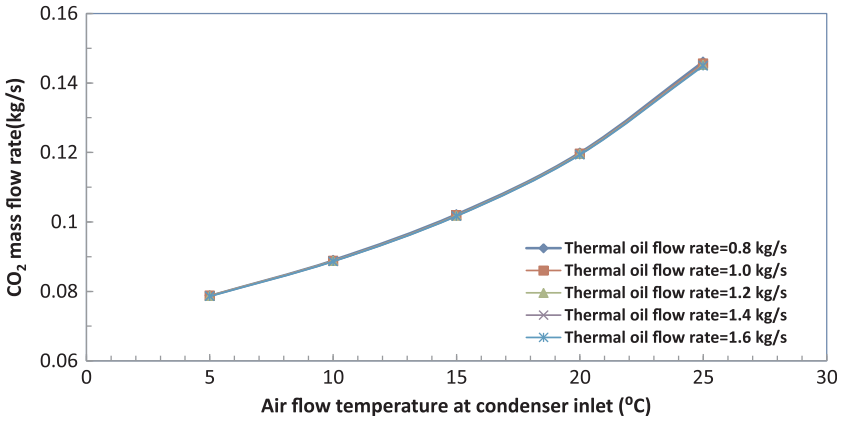

Fig. 12. Variation of CO_2 mass flow rate with thermal oil flow rate and condenser inlet air Temperature.

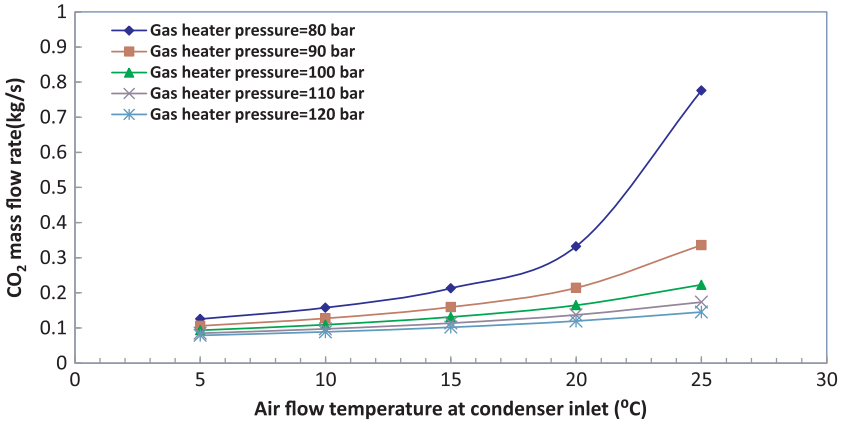

Fig. 13. Variation of CO_2 mass flow rate with CO_2 turbine inlet pressure and condenser inlet air temperature.

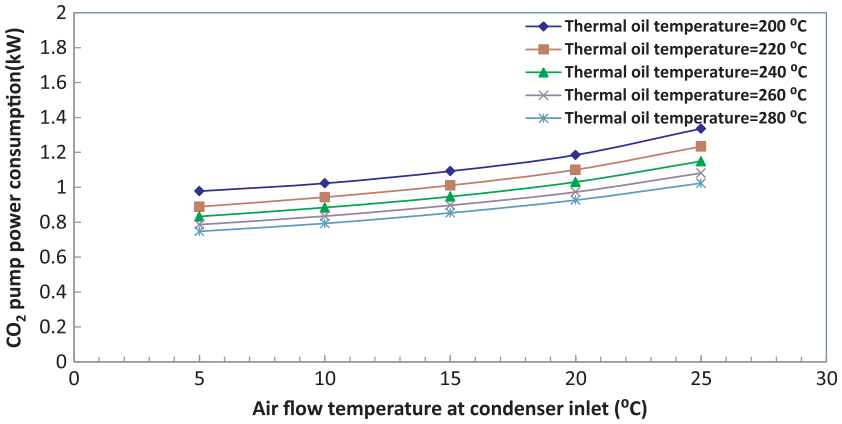

Fig. 14. Variation of CO_2 pump power consumption with thermal oil temperature and condenser inlet air temperature.

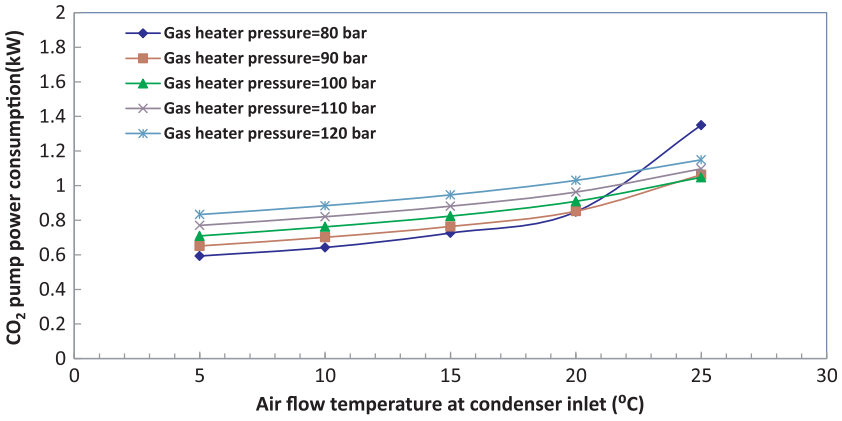

Fig. 15. Variation of CO_2 pump power consumption with CO_2 turbine inlet pressure and condenser inlet air temperature.

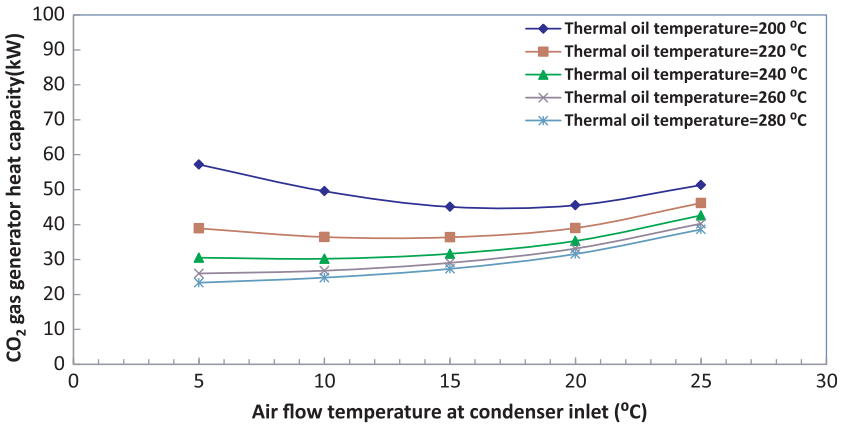

Fig. 16. Variation of CO_2 gas generator capacity with thermal oil temperature and condenserinlet air temperature.

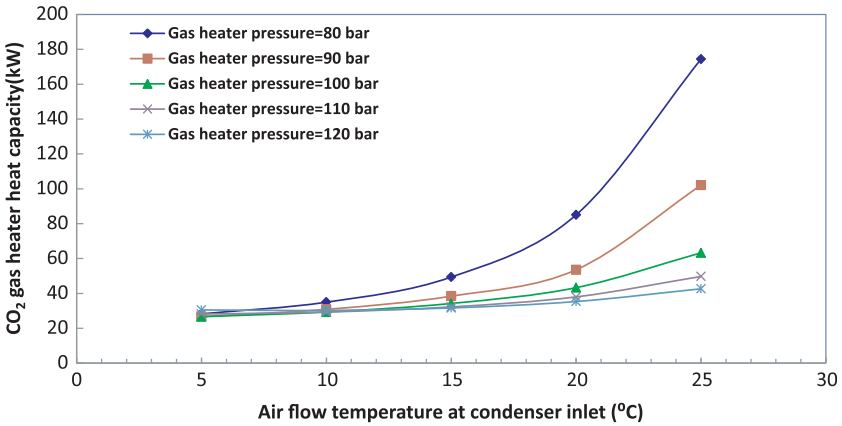

Fig. 17. Variation of CO_2 gas generator capacity with thermal oil flow rate and condenser inlet air temperature.

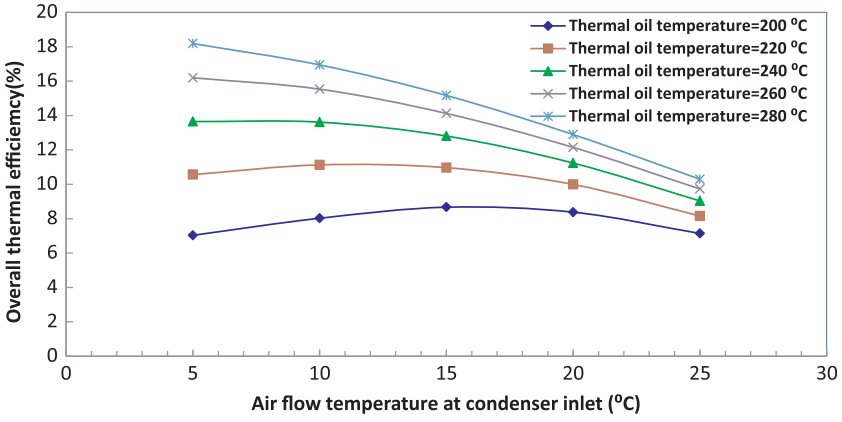

Fig. 18. Variation of system overall thermal with thermal oil temperature and condenser inlet air temperature.

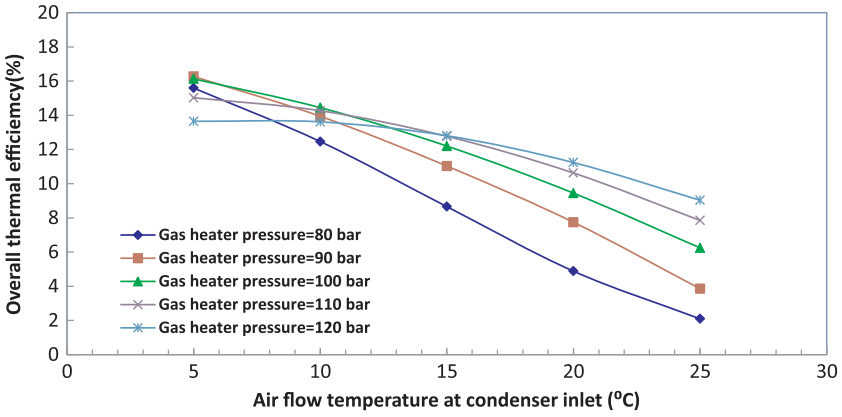

Fig. 19. Variation of system overall thermal with thermal oil flow rate and condenser inlet air temperature.

controlled to increase with ascending condenser air side temperatures but decrease with higher thermal oil temperatures when other parameters are unchanged. On the other hand, the simulation results from Fig. 12 show that thermal oil flow rates exert almost zero effect on the CO_2 mass flow rate. Moreover, in order to maintain constant power generation when the CO_2 pressure decreases from 120 bar to 80 bar, CO_2 mass flow rate should also be controlled to increase in order to maintain constant power generation, as shown in Fig. 13. In addition, if the CO_2 pressure at the turbine inlet drops to 80 bar and the condenser air inlet temperature is higher than 20 °C, a significant rise in CO_2 mass flow rate is required.

Since the CO_2 mass flow rate can be controlled by pump motor frequency or speed, this directly affects pump power consumption, as shown in Fig. 14. Subsequently, similar effects can be found for heat source parameters and condenser air temperatures on CO_2 pump power consumption. Additionally, the CO_2 pump power consumption is mainly affected by CO_2 mass flow rate and CO_2 pump pressure ratio. In this case, as shown in Fig. 15, higher CO_2 pressures at the turbine inlet require a higher CO2 pump power input when the condenser air inlet temperature is less than 20 °C. When the CO_2 mass flow rate increases abruptly at a higher air temperature and lower CO_2 pressure, a greater CO_2 pump power input is needed.

The CO_2 gas generator capacity is mainly determined by the maximum fluid temperature difference between hot and cold sides and also the CO_2 mass flow rate. In some cases, such as with low thermal oil temperatures, the effect of large temperature shifts in heat capacity can overwhelm CO_2 mass flow rates. For example, in Fig. 16, when the condenser air temperature is lower than 15 °C and thermal oil temperature is 200 °C, the heat capacity decreases at higher condenser air temperatures or higher CO_2 mass flow rates. Otherwise, at a constant thermal oil temperature, the heat capacity generally increases with higher condenser air temperatures and CO_2 mass flow rates. In the meantime, at a constant condenser air temperature, the heat capacity increases with lower thermal oil temperatures due to the requisite high CO_2 mass flow rate. On the other hand, as shown in Fig. 17, the effects of CO_2 pressure at the turbine inlet and condenser air inlet temperature on gas heater capacity are very similar to those same parameters on the CO_2 mass flow rate. At the same condenser air inlet temperature, the CO_2 gas heater heat capacity increases with lower CO_2 pressures at the turbine inlet, and the gap increases with higher condenser air inlet temperatures.

The overall system thermal efficiency is a ratio of net power generation (CO_2 power generation minus pump power consumption) to gas generator heat capacity. Since the system power generation is fixed at 5 kW, thermal efficiency is determined solely by CO_2 pump power consumption and gas generator capacity. As shown in Fig. 18, at a constant thermal oil temperature of greater than 240 °C, overall thermal efficiency generally decreases with higher condenser air temperatures. But when a thermal oil temperature is lower than 240 °C, a maximum overall thermal efficiency can be obtained due to its effect on the generator heat capacity. In addition, as shown in Fig. 19, overall efficiency increases with higher CO_2 pressures at the turbine inlet when condenser air inlet temperatures are above 15 °C. However, with condenser air inlet temperatures of below 15 °C, overall efficiency tends to decrease with higher CO_2 pressures at the turbine inlet due to the increased pump power consumption.

The experimental and simulation results are beneficial to aid understanding of system performance at different applicable operating conditions and can therefore lead to optimal controls of system operation once turbine power generation is specified. The safety and efficient operations can also be controlled for the T-CO_2 systems if the research outcomes from this paper can be applied.

4. Conclusions

A transcritical CO_2 Rankine cycle (T-CO_2) is a prospective option for low temperature heat source power generation, considering its natural working fluid properties and lower footprint compared with conventional ORC systems. A small-scale test rig of the T-CO_2 Rankine cycle was developed and measurements were carried out to investigate the effects of heat source and sink parameters on system performance. Preliminary test results showed that the CO_2 mass flow rate could be directly controlled by variable CO_2 liquid pump speeds. The CO_2 pressures at the turbine inlet and outlet and turbine power generations all increased with higher CO_2 mass flow rates. In addition, the tested turbine overall efficiency proved to be smaller than its isentropic efficiency, indicating that the turbine's mechanical and electrical efficiencies need to be further improved. The heat source flow rate was also found to confer almost negligible impact on system performance. On the other hand, a model of the tested T-CO_2 power generation system has been developed by integrating all the system component models, and validated against both current measurements and previous test results. The validated model is therefore used to predict the effects of heat source and sink parameters and CO_2 pressures at the turbine inlet with larger scales on the system performance. The simulation results show that heat source, heat sink temperatures and CO_2 pressures at the turbine inlet all have significant effects on system performance. A maximum system thermal efficacy exists when the system works at certain conditions such as high pressure at the turbine inlet or low heat source temperature. In addition, the effect of heat source flow rate on system performance is relatively small. This system model can be an efficient and useful tool in the investigation of alternative system designs, efficient controls, performance evaluation and optimisation.

Acknowledgements

The authors would like to acknowledge the support received from GEA Searle, Research Councils UK (RCUK) and Innovate UK for this

research project.

References

[1] Tchanche BF, Lambrinos G, Frangoudakis A, Papadakis G. Low-grade heat conversion into power using organic Rankine cycles – a review of various applications. Renew Sustain Energy Rev 2011;15(8):3963–79.

[2] Hung TC, Shai TY, Wang SK. A review of organic rankine cycles (ORCs) for the recovery of low-grade waste heat. Energy 1997;22(7):661–7.

[3] Lecompte S, Huisseune H, van den Broek M, Vanslambrouck B, De Paepe M. Review of organic Rankine cycle (ORC) architectures for waste heat recovery. Renew Sustain Energy Rev 2015;47:448–61.

[4] Yamamoto T, Furuhata T, Arai N, Mori K. Design and testing of the Organic Rankine Cycle. Energy 2001;26(3):239–51.

[5] Chen H, Goswami DY, Stefanakos EK. A review of thermodynamic cycles and working fluids for the conversion of low-grade heat. Renew Sustain Energy Rev 2010;14(9):3059–67.

[6] Ge YT, Tassou SA. Thermodynamic analysis of transcritical CO_2 booster refrigeration systems in supermarket. Energy Convers Manage 2011;52:1868–75.

[7] Jiang YT, Ma YT, Li MX, Fu L. An experimental study of trans-critical CO_2 water-water heat pump using compact tube-in-tube heat exchangers. Energy Convers Manage 2013;76:92–100.

[8] Chen Y. Novel cycles using carbon dioxide as working fluid (Ph.D. thesis). Stockholm: Division of Applied Thermo dynamics and Refrigeration, Energy Department, KTH University; 2006.

[9] Kim YM, Kim CG, Favrat D. Transcritical or supercritical CO_2 cycles using both low- and high-temperature heat sources. Energy 2012;43(1):402–15.

[10] Zhang XR, Yamaguchia H, Fujima K, Enomoto M, Sawada N. Theoretical analysis of a thermodynamic cycle for power and heat production using supercritical carbon dioxide. Energy 2007;32:591–9.

[11] Ge YT, Tassou SA. Performance evaluation and optimal design of supermarket refrigeration systems with supermarket model “SuperSim”, Part I: Model description and validation. Int J Refrig 2011;34:527–39.

[12] Zhang XR, Yamaguchi H, Uneno D, Fujima K, Enomoto M, Sawada N. Analysis of a novel solar energy-powered Rankine cycle for combined power and heat generation using supercritical carbon dioxide. Renew Energy 2006;31:1839–54.

[13] Chen Y, Lundqvist P, Johansson A, Platell P. A comparative study of the carbon dioxide transcritical power cycle compared with an organic rankine cycle with R123 as working fluid in waste heat recovery. Appl Therm Eng 2006;26:2142–7.

[14] Hettiarachchia HDM, Golubovica M, Worek WM. Optimum design criteria for an organic Rankine cycle using low-temperature geothermal heat sources. Energy 2007;32(9):1698–706.

[15] Cayer E, Galanis N, Desilets M, Nesreddine H, Roy P. Analysis of a carbon dioxide transcritical power cycle using a low temperature source. Appl Energy 2009;86:1055–63.

[16] Sarkar J. Review and future trends of supercritical CO_2 Rankine cycle for low-grade heat conversion. Renew Sustain Energy Rev 2015;48:434–51.

[17] Chen H, Goswami DY, Rahman MM, Stefanakos EK. Energetic and exergetic analysis of CO_2-and R32-based transcritical Rankine cycles for low-grade heat conversion. Appl Energy 2011;88(8):2802–8.

[18] Li X, Zhang X. Component exergy analysis of solar powered transcritical CO_2 Rankine cycle system. J Therm Sci 2011;20(3):195–200.

[19] Baik YJ, Kim M, Chang KC, Kim SJ. Power-based performance comparison between carbon dioxide and R125 transcritical cycles for a low-grade heat source. Appl Energy 2011;88(3):892–8.

[20] Ge YT, Tassou SA, Dewa Santosa I, Tsamos K. Design optimisation of CO_2 gas cooler/condenser in a refrigeration system. Appl Energy 2015;160:973–81.

[21] Capra F, Martelli E. Numerical optimization of combined heat and power Organic Rankine Cycles – Part B: simultaneous design & part-load optimization. Energy 2015;90:329–43.

[22] Shah RK, Sekulic DP. Fundamentals of heat exchanger design. Inc.: John Wiley and Sons; 2003.

[23] Martin H. A theoretical approach to predict the performance of chevron-type plate heat exchangers. Chem Eng Process 1996;35:301–10.